

# The Dependence of Cloud Particle Size on Non-Aerosol-Loading Related Variables

*H. Shao and G. Liu  
Florida State University  
Tallahassee, Florida*

## Introduction

An enhanced concentration of aerosol may increase the number of cloud drops by providing more cloud condensation nuclei (CCN), which in turn results in a higher cloud albedo at a constant cloud liquid water path. This process is often referred to as the aerosol indirect effect (AIE). Many in situ and remote sensing observations support this hypothesis (Ramanathan et al. 2001). However, satellite observed relations between aerosol concentration and cloud drop size are not always in agreement with the AIE. Based on global analysis of cloud effective radius ( $r_e$ ) and aerosol number concentration ( $N_a$ ) derived from satellite data, Sekiguchi et al. (2003) found that the correlations between the two variables can be either negative, or positive, or none, depending on the location of the clouds. They discovered that significantly negative  $r_e - N_a$  correlation can only be identified along coastal regions of the continents where abundant continental aerosols inflow from land, whereas Feingold et al. (2001) found that the response of  $r_e$  to aerosol loading is the greatest in the region where aerosol optical depth ( $\tau_a$ ) is the smallest. The reason for the discrepancy is likely due to the variations in cloud macroscopic properties such as geometrical thickness (Brenguier et al. 2003). Since  $r_e$  is modified not only by aerosol but also by cloud geometrical thickness ( $H$ ), the correlation between  $r_e$  and  $\tau_a$  actually reflects both the aerosol indirect effect and dependence of  $H$ . Therefore, discussing AIE based on the  $r_e - \tau_a$  correlation without taking into account variations in cloud geometrical thickness may be misleading. This paper is motivated to extract aerosols' effect from overall effects using the independent measurements of cloud geometrical thickness,  $\tau_a$  and  $r_e$ .

## Analytical Model

To detect the true signal from the aerosol indirect effect, one must obtain the correlation between  $r_e$  and  $\tau_a$  at the same  $H$ . In order to fix  $H$ , we turn to the following analytical model. For an adiabatic cloud,  $r_e$  may be related to cloud drop number concentration ( $N_c$ ) and  $H$  by (Brenguier et al. 2003)

$$r_e \propto N_c^{-1/3} H^{1/3} \quad (1)$$

Since entrainment may dilute the cloud water and cause the cloud departing from an adiabatic cloud, we write this equation in a more general form for marine stratus:

$$r_e = A_0 N_c^{-\alpha_0} H^\beta, \quad (2)$$

where  $A_0$ ,  $\alpha_o$ , and  $\beta$  are constants. If increased  $N_a$  leads to a larger number of CCN,  $N_c$  in (2) may be replaced by  $B_0\tau_a^\gamma$ , where  $B_0$  and  $\gamma$  describes the conversion rate from aerosol particles to cloud droplets. We obtain

$$r_e = \sigma \tau_a^{-\alpha} H^\beta , \quad (3)$$

where  $\sigma = A_0 B_0^{-\alpha_0}$ ,  $\alpha = \alpha_0 \gamma$ . The exponents  $\alpha$  and  $\beta$  reflect how important the aerosol concentration and cloud depth respectively are in determining the cloud drop size.

## Data Analysis and Results

We use stratus cloud observed over the northeastern Pacific during summer (June, July and August) 2000 as an example to explain the coherent pattern problem, and further to determine AIE. Cloud effective radius, cloud optical depth and drizzle index are derived from combined visible, near-infrared and microwave data of the Tropical Rainfall Measuring Mission (TRMM) satellite (Shao and Liu 2004). To ensure that measurements are from warm, non-precipitating stratus clouds, we use the following criteria to select our dataset: 1) infrared cloud top brightness temperature between 280 K and 288 K, 2) drizzle index less than 1.0, i.e., no drizzle occurring in the clouds, and 3) the product of the variances of  $r_e$  and cloud optical depth within a TRMM Microwave Imager's (TMI) 19 GHz field of view ( $\sim 15$  km) less than  $8.0 \mu\text{m}^2$  (a threshold used to filter out non-uniform convective clouds in our study). Six-hourly NCEP/NCAR reanalysis surface data are utilized to obtain air temperature and relative humidity near surface. Using the air temperature and relative humidity, we evaluate the temperature at the lifting condensation level (LCL) by assuming air mass ascent from near surface following a dry adiabatic lapse rate. The temperature difference between LCL and cloud top (determined by infrared satellite data) is then calculated. We obtain the cloud depth by assuming an in-cloud lapse rate of  $7.5 \text{ K km}^{-1}$ . Data of aerosol optical depth used in this study are from the Moderate Resolution Imaging Spectroradiometer atmospheric aerosol product archived by NASA.

The three-monthly (June to August, 2000) geometric mean distributions of  $\tau_a$ ,  $r_e$ , and  $H$  are shown in Figure 1 (gridded every  $1^\circ \times 1^\circ$ ). One feature is that both  $\tau_a$  and  $H$  have the greatest gradient almost perpendicular to the California coastal line. The gradient of  $\tau_a$  and  $H$  has the opposite sign near coastal region (i.e.,  $H$  increases while  $\tau_a$  decreases away from the coast), but the same sign far off the coast. As a result (see Figure 2), for  $H > 5.5 \text{ km}$  (points far off the coast where the gradients of  $\tau_a$  and  $H$  have the same sign) there is little correlation between  $r_e$  and  $\tau_a$  while for  $H < 5.5 \text{ km}$  (points near the coast

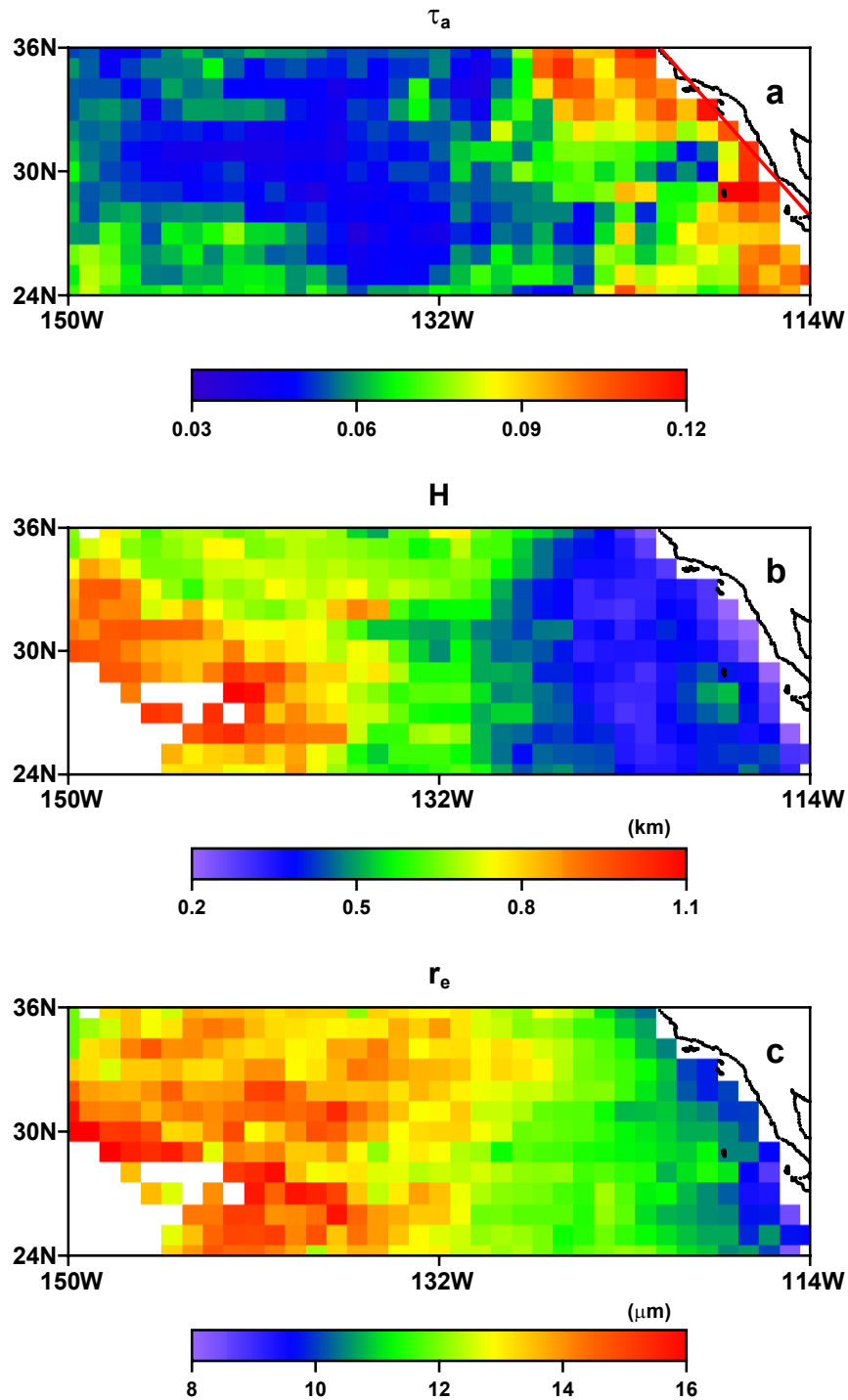


**Figure 1.** Three-monthly (June to August, 2000)  $1^\circ \times 1^\circ$  geometric mean distributions of (a) aerosol optical depth  $\tau_a$ , (b) cloud depth  $H$ , and (c) cloud effective radius  $r_e$ .

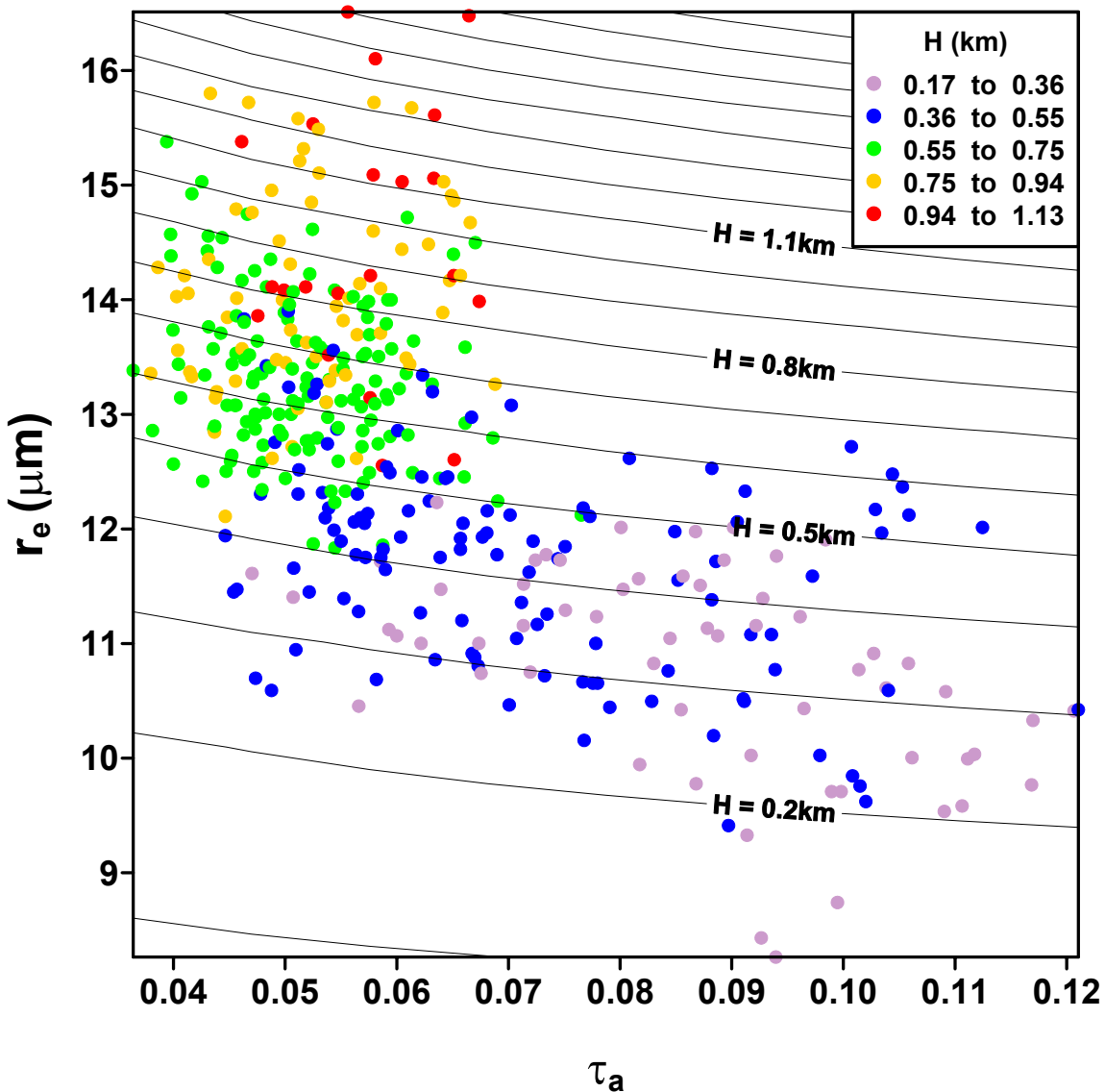


**Figure 2.** Scatter diagram of  $r_e$  and  $\tau_a$ , for observed data colored with  $H$ . The black curves show the  $r_e - \tau_a$  relation at constant values of  $H$  calculated using (3) and regressed  $\sigma$ ,  $\alpha$ , and  $\beta$  values in Table 1.

where the gradients of  $\tau_a$  and  $H$  have the opposite sign) there is strong correlation between  $r_e$  and  $\tau_a$ , indicating the coupled effects of aerosol concentration and cloud depth on cloud drop size.

To extract the aerosols' effect from overall effects the multivariate linear regression of  $\ln r_e$  on  $\ln r_e$  and  $\ln H$  is performed based on the logarithm form of (3) by using the above three-monthly geometric mean  $1^\circ \times 1^\circ$  data of  $r_e$ ,  $\tau_a$  and  $H$ . Table 1 summarizes the coefficients and R-square values of these regressions together with the width of 95% confidence interval for each coefficient (shown in the parentheses). Regression coefficients and their 95% confidence intervals indicate that the correlations between  $r_e$  and  $\tau_a$  (negative) and between  $r_e$  and  $H$  (positive) are statistically significant. The R-square value shows the multivariate regression explains 73.4% of the total variance in the observed  $r_e$ , indicating that the

**Table 1.** Summary of Regressions (Sample number = 403)

R <sup>2</sup>	Variables	Coefficients
0.734	ln $\tau_a$ ln $H$ Constant	- $\alpha$ : -0.070 ( $\pm$ 0.031) $\beta$ : 0.241 ( $\pm$ 0.023) ln $\sigma$ : 2.477

relationship described by (3) is statistically robust for our dataset. The black curves in Figure 2 show the  $r_e$  -  $\tau_a$  relation at constant values of  $H$  calculated with (3) and the regressed  $\sigma$ ,  $\alpha$ , and  $\beta$  in Table 1. The slopes of those curves are steeper than the mean slope of those points with  $H > 5.5$  km but less steeper than that of those points with  $H < 5.5$  km, implying that in the region where the gradients of  $\tau_a$  and  $H$  have the opposite sign the observed aerosol indirect effect may be overestimated, and it may be underestimated in the region where the gradients of  $\tau_a$  and  $H$  have the same sign.

## Conclusions

Using an analytical model, we explained how the coherent nature between  $H$  and  $\tau_a$  as observed in the northeastern Pacific causes misidentification of AIE. It is shown that the gradients of both variables are almost normal to the California coastline with opposite signs near the coast and the same sign far off the coast. As a result, the apparent AIE is enhanced near the coast while it is reduced far off the coast. This may explain the findings of Sekiguchi et al. (2003), who found that negative correlation between  $N_a$  and  $r_e$  is the most evident near coastal regions (including the California coastal regions), while the correlation becomes less significant or even turns to positive far off shore. Our study also manifests that in the regions where increasing aerosol loading appears to increase cloud drop size, the real AIE still works in the direction of reducing cloud drop size with the increase of aerosol loading.

## Corresponding Author

Hongfei Shao, email: [soar@met.fsu.edu](mailto:soar@met.fsu.edu), (850) 645-5629

## References

- Brenguier, JL, H Pawlowska, and L Schüller. 2003. "Cloud microphysical and radiative properties for parameterization and satellite monitoring of the indirect effect of aerosols on climate." *Journal of Geophysical Research* 108, 8632, doi:10.1029/2002JD002682.
- Feingold, G, LA Remer, J Ramaprasad, and Y Kaufman. 2001. "Analysis of smoke impact on clouds in Brazilian biomass burning regions: An extension of Twomey's approach." *Journal of Geophysical Research* 106(22)907– 22,922.
- Ramanathan, V, PJ Crutzen, JT Kiehl, and D Rosenfeld. 2001. "Aerosols, climate and the hydrological cycle, Science." 294, 2119-2124.

Sekiguchi, M, T Nakajima, K Suzuki, K Kawamoto, A Higurashi, D Rosenfeld, I Sano, and S Mukai. 2003. "A study of the direct and indirect effects of aerosols using global satellite datasets of aerosol and cloud parameters." *Journal of Geophysical Research* 108, 4699, doi:10.1029/2002JD003359.

Shao, H, and G Liu. 2004. "Detecting drizzle in marine warm clouds using combined visible, infrared, and microwave satellite data." *Journal of Geophysical Research* 109, D07205, 10.1029/2003JD004286.